Modeling the liquid–liquid extraction equilibrium of iron (III) with hydroxyoxime extractant and equilibrium-based simulation of counter-current copper extraction circuits

Vasilyev Fedor, Virolainen Sami, Sainio Tuomo

DOI: 10.1016/j.ces.2017.10.003

Revised manuscript

Manuscript number: CES-D-17-01189

Submitted to *Chemical Engineering Science*, September 19, 2017

Modeling the liquid–liquid extraction equilibrium of iron (III) with hydroxyoxime extractant and equilibrium-based simulation of counter-current copper extraction circuits

Fedor Vasilyev, Sami Virolainen, Tuomo Sainio*.

Lappeenranta University of Technology
Laboratory of Separation Technology
P.O. Box 20. FI-53851, Lappeenranta, Finland

*) Corresponding author: Prof. Tuomo Sainio, Phone: + 358 40 3578683, Email: tuomo.sainio@lut.fi

Abstract

The phase equilibrium in the loading and stripping stages of the liquid–liquid extraction of iron (III) with hydroxyoxime extractant in kerosene was studied over a wide range of hydroxyoxime extractant (Acorga M5640, 3–25 vol–%) and iron (1.5–45 g/L) concentrations. A mechanistic mathematical model explaining the phase equilibrium in the loading stage was developed and validated with new experimental data. The model accounts for the non-ideality of both the aqueous and the organic phases. The composition of the aqueous sulfate solution was calculated through speciation of the electrolytes with an extended Debye–Hückel model. The organic phase non-ideality in the loading stage was described with an empirical correlation that accounts for the effect of extractant concentration on the extraction equilibrium constant. The model parameters were fitted against measured experimental data using nonlinear regression analysis. A mechanistic mathematical model explaining the co-extraction of iron in copper liquid–liquid extraction was developed and validated using D-optimal experiment design and the Markov chain Monte Carlo algorithm. The model facilitates the optimization of copper liquid–liquid extraction circuits, as iron is the most common impurity in industrial systems, making process operations challenging.

Keywords

Liquid–liquid extraction; Iron; Equilibrium modeling; MCMC; hydroxyoxime; Acorga M5640; D-optimal design of experiments

1. Introduction

About 20% of primary copper is produced by the hydrometallurgical method, which involves the leaching of copper-bearing ores or concentrates with sulfuric acid solutions followed by liquid–liquid extraction with hydroxyoxime extractants and electrodeposition of high-purity cathode copper (Schlesinger *et al*., 2011b). Since such leaching is not selective, impurities including iron, zinc, magnesium, nickel, cobalt, and arsenic are also leached (Gotfryd and Pietek, 2013). However, the liquid–liquid extraction process produces relatively pure copper (II) sulfate solutions for electrowinning due to the high copper selectivity of the hydroxyoxime extractants used for purification and concentration. The purity requirements with respect to the content of most contaminants in copper electrolytes are not particularly high because of the position of the copper in the electrochemical series. Therefore, no special attention is paid to their levels when they occur within relatively broad but acceptable limits (Gotfryd and Pietek, 2013). This applies especially to nickel, cobalt, arsenic, and antimony. Cobalt might even be desirable in the electrolytes to prevent corrosion of insoluble lead anodes. However, the amount of iron (III) that is present in electrolytes is more strictly restricted and controlled, as its reduction at the cathode competes with the copper electrodeposition reaction. This lowers the current efficiency of copper plating (Schlesinger *et al*., 2011c).

Even though hydroxyoxime extractants have been proven to be very selective towards copper (Szymanowski, 1993; Kabugo *et al*., 2017), the transfer of iron (III) and other impurities from the pregnant leach solution (PLS) to rich electrolytes (RE) is inevitable (Gotfryd and Pietek, 2013; Molnar and Verbaan, 2003). Most of the iron (III) transfer is due to chemical extraction, while entrainment contributes to a minor extent (Thomas, 2010). The buildup of impurities in the electrolyte is controlled by bleeding a small portion of the electrolyte from the tank house, which increases operational costs. Therefore, the transfer of impurities and especially of iron (III) must be minimized. This can be done through the accurate selection of an extractant formulation that can provide high enough selectivity with regard to iron (III) and other impurities as well as careful design of the liquid–liquid extraction process. Mechanistic mathematical modeling of iron (III) co-extraction may serve for the latter purpose.

The liquid–liquid extraction of metals with hydroxyoxime extractants is generally presented as interfacial, reversible, and competitive reactions of metal cations and protons on the aqueous side, with chelating cation exchange extractant molecules on the organic side. Depending on the extracting selectivity, one of the metal cations is extracted selectively over others. The

extraction of iron (III) in the range of low aqueous iron concentrations with hydroxyoxime extractants has been studied and reported in the literature (Aminian and Bazin, 2000; Ocaña and Alguacil, 1998; Parus *et al*., 2011; Simpson *et al*., 1996; Zhang *et al*., 2016). However, the data on extraction in a wide range of conditions, especially in the range of high aqueous iron (III) concentrations, remain insufficient. Agarwal *et al*. (2012), Aminian and Bazin (2000), Ocaña and Alguacil (1998), and Simpson *et al*. (1996) studied the effect of the presence of iron (III) in the aqueous solution on the extraction of copper, when copper was extracted preferably. Iron (III) was found to have a minor effect on copper extraction. However, there were no attempts to quantify how much iron (III) is actually co-extracted with copper under different extraction conditions. Even so, the information is critical for copper liquid–liquid extraction process design, as it is important to predict under which process operation conditions the iron (III) transfer from the PLS to RE is minimized. In sum, there is no model available in the literature that allows the prediction of the equilibrium composition of the process phases of the liquid–liquid extraction of copper in the presence of iron (III) with a hydroxyoxime extractant in wide PLS and extractant concentration ranges.

In this work, a mechanistic mathematical model explaining the equilibrium of iron (III) liquid–liquid extraction in wide ranges of iron (III) and hydroxyoxime extractant concentrations was correlated. The developed mechanistic model was verified with new experimental data on the equilibrium of the loading stage. This model was then combined with a previously developed model for copper liquid–liquid extraction equilibrium (Vasilyev *et al*., 2017). The combined model was verified with experimental data collected using D-optimal experiments. The verified combined model was then used to optimize a copper liquid–liquid extraction circuit, with the aim to minimize iron (III) transfer from PLS to RE.

2. Materials and methods

2.1. Materials

The extractant employed in this study was Acorga M5640 (Cytec), with an active substance of 2-hydroxy-5-nonylsalicylaldoxime. It was used after washing two times with 3 M H_2SO_4. The washed organic as well as samples taken from the batch equilibrium experiments were centrifuged for 10 min at 4000 rpm prior to analyses to ensure complete phase disengagement. Aliphatic kerosene Exxsol D80 (Exxon Mobil) was used as a diluent. Aqueous stock solutions of iron (III) and copper (II) were prepared by dissolving exsiccated iron (III) sulfate (Sigma–

Aldrich, AR grade) and copper (II) sulfate (VWR Chemicals, AR grade) in purified water (Elga Veolia Centria R120). The acidity was adjusted with H_2SO_4 (Merck, AR grade).

2.2. Experimental procedure

Extraction and stripping experiments were carried out on an orbital shaker in 50 mL separation funnels, with a 30 min equilibration time at 20 °C. The contact time was chosen based on data presented elsewhere (Ocaña and Alguacil, 1998; Simpson *et al*., 1996). The organic to aqueous (O/A) phase ratios were varied. In the loading experiments, aqueous phases with known iron and copper contents and acidity were contacted with the metal-free organic phases of known extractant concentrations. In the stripping experiments, metal-free aqueous phases of known acidity were contacted with the loaded organic phases with known metals and extractant concentrations.

The design of the experiments to study the extraction and stripping equilibrium of iron (III) is shown in Table 1. One-factor-at-a-time strategy was used in the experimental designs aiming at collecting sufficient data to visually assess the influences of the variable experimental conditions on iron extraction equilibrium and to fit a model predicting the equilibrium. In all the extraction (E1–E9) and stripping (S1–S5) experiments, only the O/A was varied, keeping the initial phases composition constant. The equilibrium acidity was not controlled in all the experiments. The loaded organic phases for the stripping experiments (S1–S5) were prepared by contacting fresh organic phases of known extractant concentrations with an aqueous phase containing 39 g/L of iron (III) at a pH of 1.06. The loaded organic phases were typically stored overnight before the stripping experiments. Each experiment was replicated twice. The equilibrium iron concentration and equilibrium pH in the aqueous phase were measured. The iron concentration in the organic phase was calculated from mass balance. Volume changes due to mixing were neglected.

Iron and copper content in the aqueous phase was analyzed via ICP–MS (Agilent technologies, Agilent 7900). A Mettler Toledo T50 titrator with a DG 111–SC electrode was used to measure the total free oxime concentration in the metal free organic phases with the ultimate loading method using a standard 0.1 M NaOH solution (Sigma–Aldrich, AR grade). Measurements of the pH were carried out with a Consort C3010 pH meter using a SenTix Mic glass electrode.

Table 1. Experimental designs of the extraction and stripping experiments. Subscript 0 refers to the initial solutions.

Extraction	Initial Fe loading = 0%.				
Experiment set ID	C_0(Fe), g/L	pH_0	$C_0(H_2SO_4)$, g/L	HR, M	O/A range
E1	1.45	1.65	1.57	0.18	1/10 … 10/1
E2	23.27	1.19	1.57	0.18	1/10 … 10/1
E3	23.27	1.19	1.57	0.50	1/10 … 10/1
E4	23.55	1.17	0.54	0.19	1/10 … 10/1
E5	3.02	1.84	0.39	0.19	1/10 … 10/1
E6	3.02	1.84	0.39	0.50	1/10 … 10/1
E7	3.07	1.81	0.16	0.19	1/10 … 10/1
E8	3.07	1.81	0.16	0.50	1/10 … 10/1
E9	16.13	1.36	0.16	0.50	1/10 … 10/1
E10	16.13	1.36	0.16	0.19	1/10 … 10/1
E11	3.07	1.81	0.39	0.30	1/10 … 10/1
E12	3.17	1.81	0.39	0.05	1/10 … 10/1
E13	45.37	0.82	0.16	0.23	1/10 … 10/1

Stripping	C_0(Fe) = 0 g/L			
Experiment set ID	$C_0(H_2SO_4)$, g/L	HR, M	Initial Fe loading, %	O/A range
S1	130	0.22	56	1/10 … 10/1
S2	160	0.22	56	1/10 … 10/1
S3	190	0.22	56	1/10 … 10/1
S4	160	0.31	36	1/10 … 10/1
S5	160	0.11	47	1/10 … 10/1

2.3. Numerical methods, parameter estimation, and model selection

The model of the liquid–liquid extraction phase equilibrium consists of non-linear algebraic equations for the equilibrium constants of all the reactions in the assumed mechanism and of mass balance equations for the elements in the system. In addition, a semi-empirical equation is used to account for aqueous phase non-ideality by correcting the equilibrium constants of the aqueous phase reactions. A rate-based approach (Kuitunen, 2014; Salmi *et al.*, 2011) is used to solve the model equations in the same manner as reported elsewhere (Vasilyev *et al.*, 2017).

Unknown model parameters are estimated by non-linear regression fitting of experimentally measured total iron concentrations in the aqueous phase, minimizing the weighted sum of squared residuals (Eq. (1)).

$$Res = \sum_{g=1}^{G}\sum_{j=1}^{N}\left(\frac{Y_j^{exp} - Y_j^{mod}}{max\left(Y_{g,j}^{exp}\right)}\right)^2, \quad (1)$$

where *Res* is the weighted sum of squared residuals, *Y* is the total equilibrium molar concentration of iron, j is the number of experiments, N is the total number of experiments in the experimental group, *g* is the number of groups, and G is the total number of experimental groups.

Since the range of the measured values of the total concentrations was very wide, giving high weights to some experimental results while disregarding others, the experimental data were weighted inside the data groups (E1–E13 or S1–S5). Hence, the data from different groups had equal importance in the estimation of the model parameters.

Selection of the most appropriate model for the iron liquid–liquid extraction equilibrium in our study was done according to the following principle: the model with the minimum mean squared error (MSE; Eq. (2)), explaining the experimental data well enough according to visual observations of the loading isotherms, and with the minimum number of parameters is preferable (Beck and Arnold, 1977).

$$MSE = \frac{Res}{N - p}, \quad (2)$$

where *p* is the number of fitted parameters in the model.

All modeling in the current study has been done in Matlab. An open source MCMC code package developed by Laine (2015) was used for estimating the reliability of the modeling results.

2.4. Model-based D-optimal design of experiments

Since the capability of a model to represent a physical system must ultimately be assessed by comparing the model's predictions with actual measured behavior, the combined model for predicting the extraction of copper and iron from mixed aqueous solutions has to be validated

against experimental data. The technique of design of experiments (DoE), which is an important link between the experimental and modeling worlds, was used for that purpose. The use of DoE here is intended to obtain the maximum information from an experimental apparatus being modeled by devising experiments that will yield the most informative data, in a statistical sense, for use in the model validation (Franceschini and Macchietto, 2008). Since parameter estimates for the equilibrium constants of the extraction reactions of copper and iron are the most critical for the model validity, D-optimal DoE, which minimizes the volume of confidence region for all the parameters, was selected for choosing the conditions for the test experiments. The number of experiments was arbitrarily chosen to be 15 to minimize the the laboratory workload while collecting a sufficiently large amount of data.

D-optimality minimizes the determinant of the variance–covariance matrix (Eq. (3)) that contains partial derivatives of the model response with respect to the model parameters under certain experimental conditions (Franceschini and Macchietto, 2008). The sensitivities are calculated at each experimental point, and the process is iterative. One has to sort out many experimental designs, **X**, to find the one that minimizes the function (Eq. (4)) at a fixed parameters estimate, $\hat{\boldsymbol{\theta}}$. This is a hard combinatorial problem that can be solved, for example, using the Markov chain Monte Carlo (MCMC) algorithm (Haario *et al*., 2006).

$$var\,\hat{\boldsymbol{\theta}} \sim (\boldsymbol{J}^T\boldsymbol{J})^{-1}, \tag{3}$$

$$\min M(\mathbf{X}, \hat{\boldsymbol{\theta}}) = min\left[-log\left(det(\boldsymbol{J}^T\boldsymbol{J})\right)\right], \tag{4}$$

where $\boldsymbol{J} = f(\mathbf{X}, \hat{\boldsymbol{\theta}}) = \frac{\partial \boldsymbol{\eta}(\mathbf{X}, \hat{\boldsymbol{\theta}})}{\partial \boldsymbol{\theta}}$ – the sensitivity of the responses to the parameters, $\boldsymbol{\eta}(\mathbf{X}, \hat{\boldsymbol{\theta}})$ – the model, which consists of equations describing how the equilibrium concentrations depend on the experimental conditions, **X** (initial phase compositions and O/A phase ratios), and parameters estimate, $\hat{\boldsymbol{\theta}}$.

In our case, validation of the combined model using D-optimal DoE consisted of the following steps: development of the model with the parameters estimated from the individual extraction experiments, definition of the design space (ranges of allowed experimental conditions), actual design of the experiments using the MCMC algorithm, collection of experimental data according to the DoE, and comparison of the modeling results with the experimental data.

3. Results and discussion

3.1. Speciation in the system $Fe_2(SO_4)_3$–H_2SO_4–H_2O

The electrolyte speciation in concentrated aqueous solutions can be determined using appropriate equilibrium constants and ionic activity coefficient models derived from the Debye–Hückel theory (Casas *et al.*, 2005; Cifuentes *et al.*, 2006; Yue *et al.*, 2014). In the system $Fe_2(SO_4)_3$–H_2SO_4–H_2O, the aqueous solution contains ions that are products of the dissociation reactions (Eq. (5–9)) presented in Table 2. The values of the corresponding reaction equilibrium constants are taken from the literature (Casas *et al.*, 2005; Tamminen *et al.*, 2013; Yue *et al.*, 2014). The equilibrium constants for the dissociation reactions of sulfuric acid and ferric sulfate were set to be very small, log$K$ = –3, to represent complete dissociation of the substances.

Table 2. The dissociation reactions included in the model for the aqueous phase speciation in the solutions containing copper and ferric sulfates in sulfuric acid.

Chemical reaction	Equation for equilibrium constant	log$K$	
$H^+ + HSO_4^- = H_2SO_4$	$K_1 = \frac{[H_2SO_4]}{[H^+][HSO_4^-]}$	-3	(5)
$H^+ + SO_4^{2-} = HSO_4^-$	$K_2 = \frac{[HSO_4^-]}{[H^+][SO_4^-]}$	1.98	(6)
$Fe^{3+} + SO_4^{2-} = FeSO_4^+$	$K_3 = \frac{[FeSO_4^+]}{[Fe^{3+}][SO_4^{2-}]}$	4.04	(7)
$Fe^{3+} + 2SO_4^{2-} = Fe(SO_4)_2^-$	$K_4 = \frac{[Fe(SO_4)_2^-]}{[Fe^{3+}][SO_4^{2-}]^2}$	5.38	(8)
$2Fe^{3+} + 3SO_4^{2-} = Fe_2(SO_4)_3$	$K_5 = \frac{[Fe_2(SO_4)_3]}{[Fe^{3+}]^2[SO_4^{2-}]^3}$	-3	(9)
$Cu^{2+} + SO_4^{2-} = CuSO_4$	$K_6 = \frac{[CuSO_4]}{[Cu^{2+}][SO_4^{2-}]}$	2.36	(10)

The pH of solutions in copper liquid–liquid extraction is usually below 2, as lower acidity leads to poorer extractant selectivity (Gotfryd and Pietek, 2013; Molnar and Verbaan, 2003; Ochromowicz and Chmielewski, 2013) and because a higher pH will lead to the formation of iron hydroxyl complexes and even iron precipitates (Yue *et al.*, 2014). Speciation calculations indicate that iron hydroxide complexes always play a minor role in solutions where pH is

around or below 2. As a result, at high acidities of interest (pH generally less than 2.0), the hydrolysis of ferric ions was not taken into account in the current study.

The extended Debye–Hückel model, Eq. (11), is used here to model the aqueous phase non-ideality.

$$\log \gamma_i = \frac{-Az_i^2\sqrt{I}}{1 + \mathring{a}_i B\sqrt{I}} + \dot{B}I, \qquad (11)$$

where $\mathring{a}_i$ is the hard-core diameter of the i-th ionic species, z_i is the charge of the i-th species, A and B are the Debye–Hückel parameters, and I is the ionic strength of the electrolyte solution.

This is a modification of the classical Debye–Hückel model, and it is valid for binary interactions. In order to correct the activity coefficient for those cases where molecular interactions—other than electrostatic ones—come into play, the same value in the $\dot{B}$ parameter is included for all participating species. The model is valid for aqueous electrolyte solutions with moderate (up to I = 1 M) ionic strength (Casas *et al*., 2000; Casas *et al*., 2005). The model has three temperature-dependent parameters, A, B, and $\dot{B}$, whose values at room temperature are 0.5114 $kg^{0.5}/mol^{0.5}$, 0.3288 $kg^{0.5}/mol^{0.5}/Å$, and 0.0410 kg/mol, respectively, and one parameter for each of the species, the "hard–core diameter," $\mathring{a}$.

Figure 1 shows the calculated distribution of species using the extended Debye–Hückel model and the speciation reactions (Table 2) for the system $Fe_2(SO_4)_3$–H_2SO_4–H_2O at 20°C and various concentrations of sulfuric acid and ferric ion. The calculations indicate that the $FeSO_4^+$ and $Fe(SO_4)_2^-$ are predominant iron species in the system. The relative concentration of ferric ion decreases with an increase of total iron concentration; the maximum relative concentration of ferric ion in the considered conditions is at the lowest total iron concentration (0.1 g/L) and amounts to 6% of all the iron in the system (Figure 1A). When the concentration of sulfuric acid is variable, the relative concentration of ferric ion increases with an increase of acidity (Figure 1B). However, the relative concentration of ferric ion is still very small: 3.4% at 20 g/L of sulfuric acid.

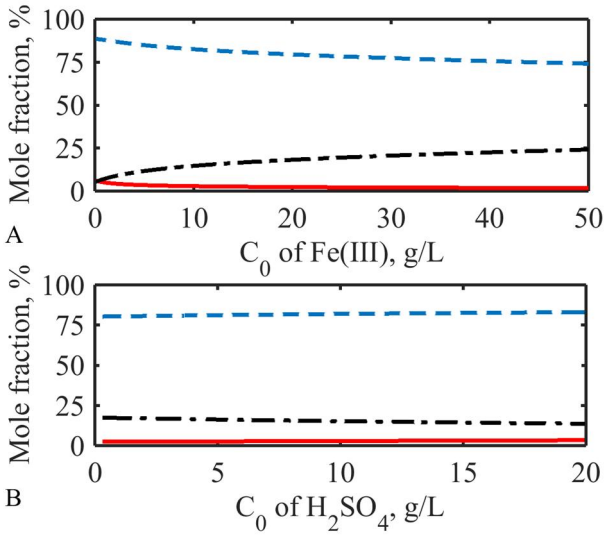

Figure 1. Calculated speciation of ferric sulfate in H_2O–H_2SO_4 system at 20 °C. A. The concentration of sulfuric acid is 1.6 g/L and that of ferric ion is variable 0.1–50 g/L; B. The concentration of sulfuric acid is variable 0.32–20 g/L and that of ferric ion is 15 g/L. Red solid lines – Fe^{3+}, blue dashed lines – $FeSO_4^+$, black dash-dot lines – $Fe(SO_4)_2^-$.

3.2. Modeling of the loading stage

Liquid–liquid extraction of a given metal by an acidic extractant is the ion transfer between the aqueous and organic phases according to an overall equilibrium reaction (Flett *et al.*, 1973; Ritcey and Ashbrook, 1984):

$$Me^{n+} + n\overline{HR} \rightleftarrows \overline{MeR_n} + nH^+. \quad (12)$$

In the case of iron (III), the overall extraction reaction takes the form shown in Eq. (13), which leads to the expression of the concentration-based extraction equilibrium constant, Eq. (14).

$$Fe^{3+} + 3\overline{HR} \rightleftarrows \overline{FeR_3} + 3H^+, \quad (13)$$

$$K_{LLX}^{Fe} = \frac{[\overline{FeR_3}]\cdot[H^+]^3}{[Fe^{3+}]\cdot[\overline{HR}]^3}. \quad (14)$$

When concentrations of species in both phases are small (ideal solutions), the equilibrium of copper extraction is traditionally described and analyzed by slope analyses using a simple linear regression model derived from Eq. (14) (Ritcey and Ashbrook, 1984):

$$\log D = \log(K_{LLX}^{Fe}) + 3 \cdot \log[\overline{HR}] + 3 \cdot pH, \quad (15)$$

where $D = [\overline{FeR_3}] / \sum[Fe^{3+}]$. A linear relationship of log$D$ vs. equilibrium pH and $\log[\overline{HR}]$ should be observed with a slope of 3, which shows the stoichiometry of the extraction reaction, whereas the intersection term gives an estimate for the extraction equilibrium constant, K_{LLX}^{Fe} (Ocaña and Alguacil, 1998; Simpson *et al*., 1996; Szymanowski, 1993). However, due to the non-ideality of the aqueous and organic phases, there are considerable deviations from Eq. (15) in systems with high and variable salinity and extractant concentrations (Rydberg *et al*., 2004; Szymanowski, 1993).

In the present study, the liquid–liquid extraction of iron (III) from sulfuric acid solutions with hydroxyoxime extractant Acorga M5640 in the aliphatic diluent Exxsol D80 was studied through 126 phase equilibrium experiments (experimental design in Table 1). Figure 2 shows that a simple linear regression model, Eq. (15), which is usually used to analyze the equilibrium in ideal solutions, is unable to explain all the variation in the collected experimental data. The deviation from the straight line of slope 3 increases with an increase of the initial total iron (III) concentration in the aqueous phase. An underlying reason is likely non-ideality of both the aqueous and organic phases since the concentrations are rather high at many of the data points. This kind of behavior was also observed with similar wide concentration range modeling of copper liquid–liquid extraction (Vasilyev *et al*., 2017).

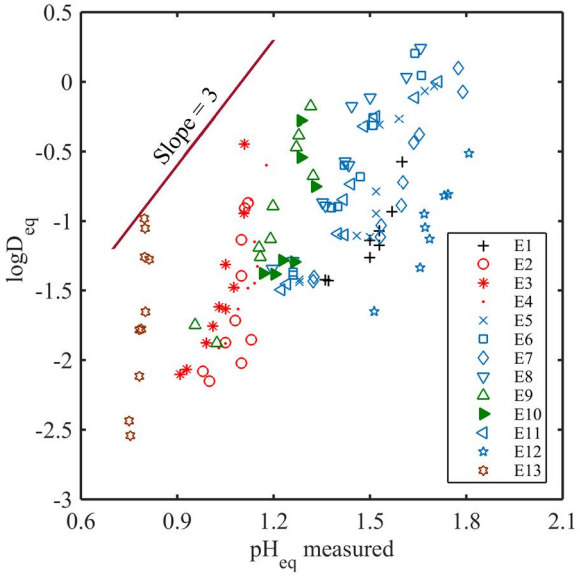

Figure 2. The equilibrium distribution of iron (III) at different equilibrium pH levels and under different experimental conditions.

Since the predominant species in the aqueous phase are $FeSO_4^+$ and $Fe(SO_4)_2^-$, the presence of sulfate ions in the aqueous solution after stripping of the loaded with iron organic phase with hydrochloric acid was checked using ion chromatography (Thermo Scientific Dionex ICS-1100 with Dionex AS-DV autosampler); no sulfate ions were detected. In addition, the presence of ferrous iron in the aqueous solutions was checked using capillary electrophoresis (Beckman Coulter P/ACE™ MDQ); likewise, no ferrous iron was detected. Therefore, based on the analysis, we assume that in the studied conditions, all iron was present in the trivalent form.

3.2.1. Mechanistic models

A mechanistic model for liquid–liquid extraction of iron, which was considered to explain the collected experimental data in this work, contains equations for aqueous speciation (Eq. (5), Eq. (6), Eq. (7), Eq. (8), Eq. (9), and Eq. (11)) and an equation for the extraction equilibrium constant, Eq. (14). When the model parameter extraction equilibrium constant, K_{LLX}^{Fe}, was estimated using all the data sets (E1–E13 in Table 3), the value of the parameter estimate, K_{LLX}^{Fe} = 0.0036, was not significant (p−value = 0.19 > 0.05). On the other hand, Figure 3 indicates an acceptable goodness of fit. The low extraction percentages of iron hinder the estimation of a significant value of the parameter.

Table 3. Dependency of the iron (III) liquid–liquid extraction equilibrium constant in the loading stage on total extractant concentration.

Experiment set ID	K_{LLX}^{Fe}	t-stat	p-value	Number of observations	MSE
E1–E13	0.0036	1.32	0.19	126	0.0028
E1	0.0096	1.99	0.08	10	0.0016
E2	0.0029	1.35	0.21	10	0.0001
E3	0.0002	1.50	0.17	10	0.0002
E4	0.0169	1.57	0.15	10	0.0002
E5	0.0135	0.21	0.84	10	0.0021
E6	0.0017	0.40	0.70	10	0.0009
E7	0.0123	0.22	0.83	10	0.0017
E8	0.0020	0.28	0.78	10	0.0017
E9	0.0016	0.68	0.51	10	0.0012
E10	0.0078	0.45	0.67	7	0.0004
E11	0.0030	0.28	0.79	10	0.0013
E12	0.1037	0.29	0.78	9	0.0003
E13	0.0004	1.34	0.21	10	0.0001

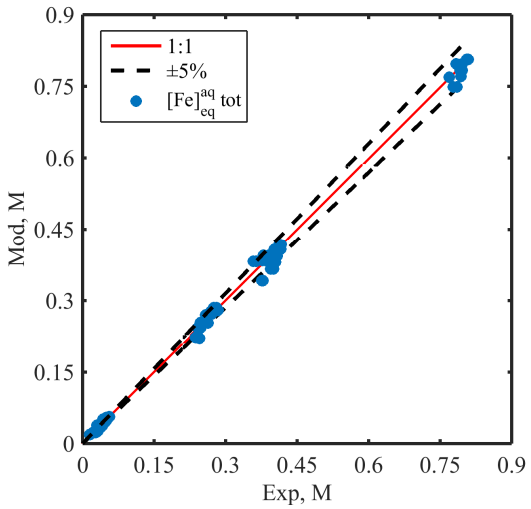

Figure 3. Goodness of fit of the iron (III) liquid−liquid extraction model in the experiments with uncontrolled equilibrium acidity. Simultaneous fitting for experimental sets E1−E13.

3.2.2. Empirical correction for organic phase non-ideality

It was observed that the value of the equilibrium constant of the extraction reaction, Eq. (14), changed when fitted individually against each data set depending on the initial composition of the process phases (Table 3). The value of the extraction equilibrium constant, K_{LLX}^{Fe}, was different in all cases, varying from 0.0002 to 0.1036. The p-value in all the cases was higher

than 0.05, indicating the low significance of the parameter estimates in all the cases. One reason for this might lie in the low number of data points in each data set. However, the fact that even the value of the parameter estimated using all the data was not significant indicated that there was a dependence that was not included in the model.

Correlation of the extraction equilibrium constant with the initial iron concentration and acidity in the aqueous phase was analyzed along with the total extractant concentration in the organic phase. The strongest correlation observed was that of the equilibrium constant and the total extractant concentration (−0.55 correlation coefficient). No other correlations among other experimental conditions were found to be significant. The same trend of a decreasing equilibrium constant with an increase of extractant concentration was reported by Hu *et al*. (2000), Lin *et al*. (2002), and Vasilyev *et al*. (2017) in the liquid−liquid extraction of copper with hydroxyoxime extractants. The behavior was explained through the non-ideality of the organic phase in all these cases.

Vasilyev *et al*. (2017) suggested the use of a hyperbolic tangent function, $K_{LLX}^{Fe} = K_{LLX,0}^{Fe} \cdot (1 - \tanh(A \cdot [HR]_{tot}))$, to take into account the correlation between the extraction equilibrium constant and the total extractant concentration in the organic phase. The two parameters, $K_{LLX,0}^{Fe}$ and A, were estimated using the whole data set (E1−E13), and significant values were obtained using the MCMC algorithm. The goodness of fit for the model, corrected for the organic phase non-ideality extraction equilibrium constant, is presented in Figure 4, which indicates acceptable modeling results.

Table 4. The parameters of the correction function for the model predicting equilibrium in the liquid–liquid extraction of iron (III).

Parameter	Estimate	Estimated 95% CI	Estimated SE	t-stat	p-value
$K_{LLX,0}^{Fe}$	0.0215	(0.015–0.028)	0.003–	6.24	6.35e-9
A	3.342	(1.575–5.110)	0.893	3.74	2.77e-4

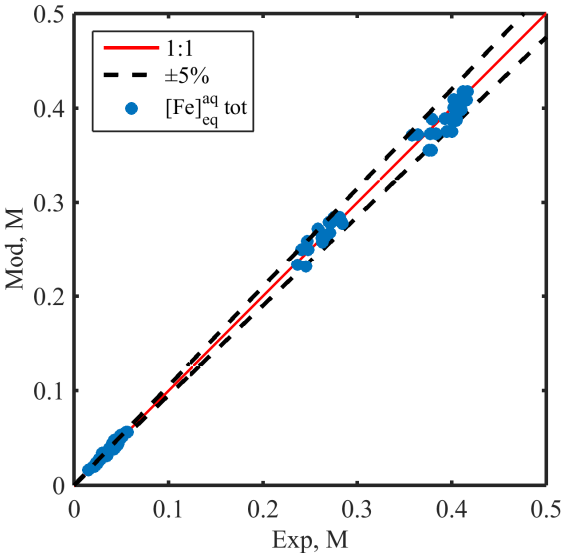

Figure 4. Goodness of fit of the iron (III) liquid−liquid extraction model with non-ideality correlated for the organic phase. The experiments were performed with uncontrolled equilibrium acidity. Simultaneous fitting for experimental sets E1−E13.

3.3. Stripping stage modeling

Since modeling the loading stage of the iron liquid–liquid extraction with aqueous speciation and a corrected extraction reaction equilibrium constant gives an excellent result, the same approach was attempted to model the equilibrium of the stripping stage of the process. The data on the stripping stage were collected according to the experimental plan presented in Table 1. There were ten equilibration experiments in each of the five data sets. Figure 5A presents the equilibrium stripping isotherms of iron, where only the O/A phase ratio was variable in each data set. The higher the phase ratio, the higher the aqueous iron concentration that can be achieved; however, only a small portion of the iron loaded onto the organic phase can actually be stripped in a single stripping stage, as indicated in Figure 5B. Even the acid concentration had little effect on the stripping efficiency. The results confirm that the stripping of iron (III) with concentrated sulfuric acid is difficult (Yu *et al.*, 1989). The reason for this is that iron (III) forms polynuclear complexes with the extractant molecules in the bulk organic phase (Smith *et al.*, 2003), and the polynuclear complex iron cannot enter the interface between the aqueous and organic phases. Special measures such as the addition of reducing agents to the stripping acid (Liu *et al.*, 2014) or utilization of oxalic acid as a stripping agent (Zhang *et al.*, 2016) may be needed to improve the stripping efficiency. However, development of a method

for the complete stripping of iron (III) from a loaded hydroxyoxime extractant is beyond the scope of the current study.

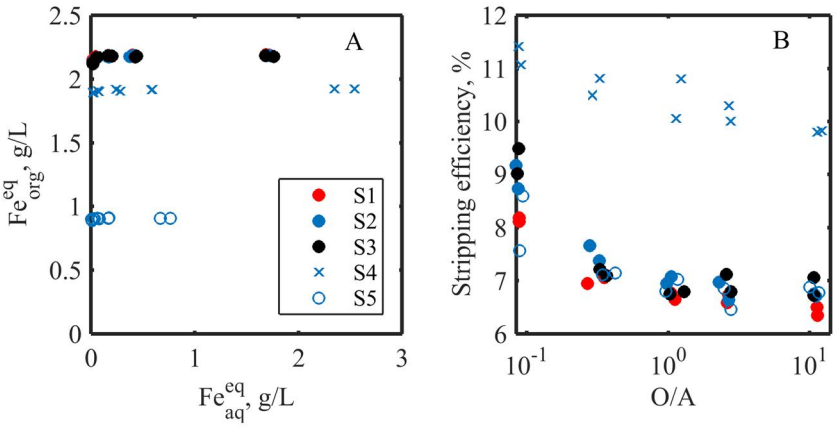

Figure 5. A. Stripping isotherms collected in the experiments with uncontrolled equilibrium acidity. B. Efficiency of stripping in the experiments with uncontrolled equilibrium acidity. Red symbols – $C_0(H_2SO_4)$ = 130 g/L , blues symbols – $C_0(H_2SO_4)$ = 160 g/L , black symbols – $C_0(H_2SO_4)$ = 190 g/L, open circles – [HR]tot = 0.11 M, filled circles – [HR]tot = 0.22 M, and crosses – [HR]tot = 0.31 M. (For interpretation of the references to color in this figure legend, the reader is referred to the web version of this article.)

Attempts were made to fit the extraction equilibrium constant for the same model as for the loading stage against the collected experimental data individually for each set of data points, with a given total extractant concentration and acidity of the aqueous phase and for the whole data set. These attempts to fit the model were not successful. Typically, some 10% of the iron (III) loaded onto the organic phase can be expected to be stripped in back-extraction under the studied conditions (Figure 5B).

3.4. Modeling of simultaneous copper and iron liquid–liquid extraction

In the case of the extraction of copper from single-metal aqueous solution by a hydroxyoxime extractant, the overall extraction reaction, Eq. (16) (Flett *et al.*, 1973), leads to the expression of the concentration-based extraction equilibrium constant, Eq. (17) (Vasilyev *et al.*, 2017). The extraction equilibrium constant takes the form $K_{LLX}^{Cu} = 50.23 \cdot (1 - \tanh(3.16 \cdot [HR]_{tot}))$, taking into account organic phase non-ideality. However, scant data are available on the modeling of liquid–liquid extraction equilibrium of copper in the case of extraction from aqueous solutions containing impurities such as iron (III) (Agarwal *et al.*, 2012; Ocaña and Alguacil, 1998; Simpson *et al.*, 1996). Once proven models for copper and iron are available, it would be interesting to check whether they are capable of predicting the extraction

equilibrium from mixed copper–iron aqueous solutions. The models for the liquid–liquid extraction equilibrium of copper and iron were combined to check their validity in the case of multi-metal extraction systems. A model-based D-optimal design of experiments (DoE) approach was used to select the experimental conditions for the experiments on liquid–liquid extraction with a hydroxyoxime extractant from mixed aqueous solutions containing high amounts of copper and iron.

$$Cu^{2+} + 2\overline{HR} \rightleftarrows \overline{CuR_2} + 2H^+ \quad (16)$$

$$K_{LLX}^{Cu} = \frac{[\overline{CuR_2}]\cdot[H^+]^2}{[Cu^{2+}]\cdot[\overline{HR}]^2}. \quad (17)$$

Table 5 presents the developed D-optimal DoE using the MCMC algorithm. Initial aqueous phase acidity and total extractant concentration were chosen manually with the idea of using the chemicals that were readily available in the laboratory. The volumetric phase ratio, O/A, was set to be the same in all the experiments. Only initial concentrations of copper and iron in the range of 0–50 g/L of each metal in the aqueous phase were the subjects of alternation during the iterative development of the DoE using the MCMC algorithm.

Table 5. Design of experiments developed using the D-optimality criterion and MCMC algorithm.

Experiment ID	$[Cu]_0$, M	$[Fe]_0$, M	$C(H_2SO_4)_0$, g/L	$[HR]_0$, M	O/A, mL/mL
1	0.30	0.47	5	0.31	1
2	0.26	0.24	5	0.31	1
3	0.55	0.46	5	0.18	1
4	0.53	0.42	5	0.18	1
5	0.25	0.45	5	0.18	1
6	0.43	0.49	0.5	0.18	1
7	0.55	0.29	0.5	0.31	1
8	0.18	0.16	0.5	0.31	1
9	0.29	0.47	0.5	0.18	1
10	0.39	0.49	0.5	0.18	1
11	0.60	0.74	0.05	0.18	1
12	0.26	0.39	0.05	0.18	1
13	0.34	0.22	0.05	0.31	1
14	0.41	0.63	0.05	0.31	1
15	0.27	0.33	0.05	0.31	1

Figure 6A demonstrates how the D-optimal DoE, developed using the MCMC algorithm, distributed the experimental conditions in the set design space. The initial copper and iron concentrations are distributed along the diagonal line, with the highest deviation in the center of the design space. This indicates that the extraction equilibrium is the most sensitive to the value of the model parameters when the aqueous phase contains twice as many moles of copper than iron. The approach to convergence with the MCMC algorithm is shown in Figure 6B.

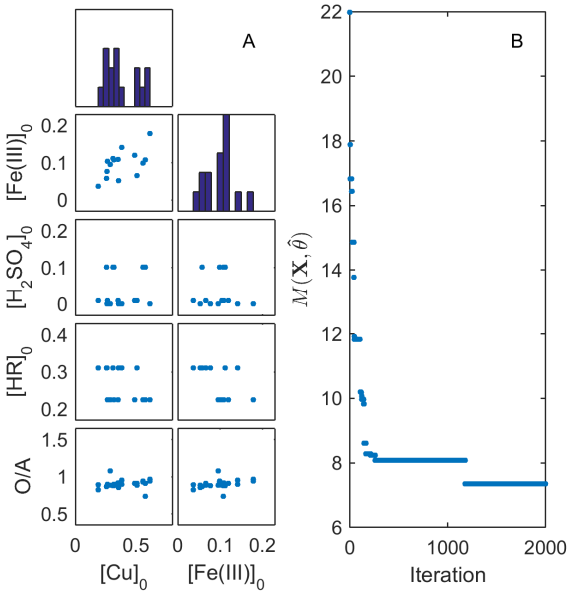

Figure 6. A. Visualization of the D-optimal DoE developed using the MCMC algorithm. B. Convergence plot.

Good prediction of the experimental data with the combined model (Figure 7) validates the ability of the model to predict the extraction equilibrium in the liquid–liquid extraction of copper with hydroxyoxime extractant in the presence of iron in the aqueous phase. It is also likely that this modeling approach would be valid with other impurities in a copper liquid−liquid extraction system.

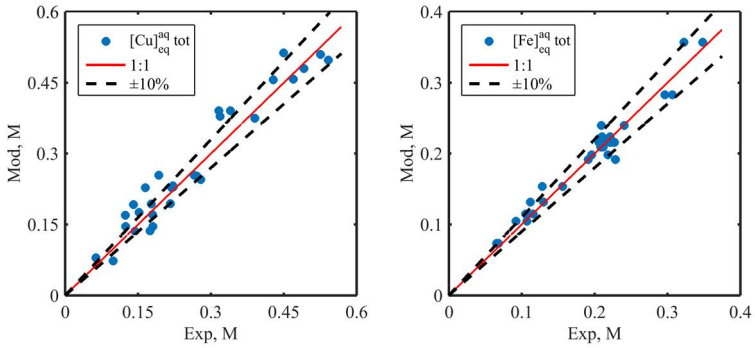

Figure 7. Comparison of experimental and modeling results for the extraction in the systems containing copper (II) and iron (III).

3.5. Equilibrium model-based study of copper liquid–liquid extraction in the presence of iron

Information on how much iron is transferred under different operational conditions, *e.g.*, relative flowrates in the process stages and extractant concentrations, is needed to optimize the performance of the copper liquid–liquid extraction process. In this section, application of the developed extraction equilibrium models for analysis of the chemical iron (III) transfer in the process is demonstrated.

While keeping the extraction circuit configuration simple (two extraction stages in series, with counter-current flow of the aqueous and organic phases and a single stripping stage, as depicted in Figure 8), the efficiency of copper transfer can be increased by increasing the extractant concentration or changing the relative flowrates of the organic and aqueous phases (the O/A ratio). However, those operational parameters influence iron transfer to the organic phase, and consequently to the RE, too. The model for simultaneous copper and iron liquid–liquid extraction that was verified in the previous section was used to simulate the extraction stages of the circuit, whereas a model for copper stripping (Vasilyev *et al.*, 2017) was used to simulate the stripping stage. Based on the iron stripping experiments (Section 3.3), it was assumed that 10% of the loaded iron is stripped.

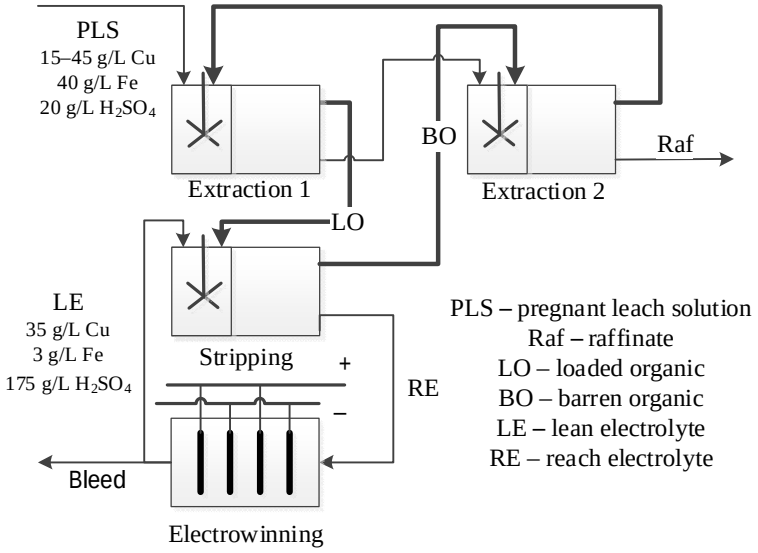

Figure 8. Process configuration used in the simulation of the iron transfer in the copper liquid–liquid extraction process. Thick and thin lines show organic and aqueous streams, respectively.

In the simulations, the PLS contained 15–45 g/L copper, 40 g/L iron, and 20 g/L H_2SO_4, which corresponds to the leach solution after pressure oxidation leaching (Schlesinger *et al.*, 2011a). The lean electrolyte (LE) coming from electrowinning back to stripping contained 35 g/L copper, 3 g/L iron, and 175 g/L H_2SO_4 (Thomas, 2010). The phase ratio (O/A) was 3.5 and 1.3 in the extraction and stripping stages, respectively. Figure 9 shows the performance of the extraction circuit depending on the copper concentration in the PLS and the extractant concentration in the organic phase. The concentration of iron in the LO increases with an increase in the extractant concentration, but it decreases with an increase of the copper content in the PLS. This is because the more free extractant (not loaded with copper) is available in organic phase, the more pronounced the extraction of iron, and consequently the larger the iron transfer to RE, as around 10% of the loaded iron is stripped in the stripping stage. Thus, the organic phase must be loaded with copper as much as possible in the extraction stage to prevent chemical iron transfer.

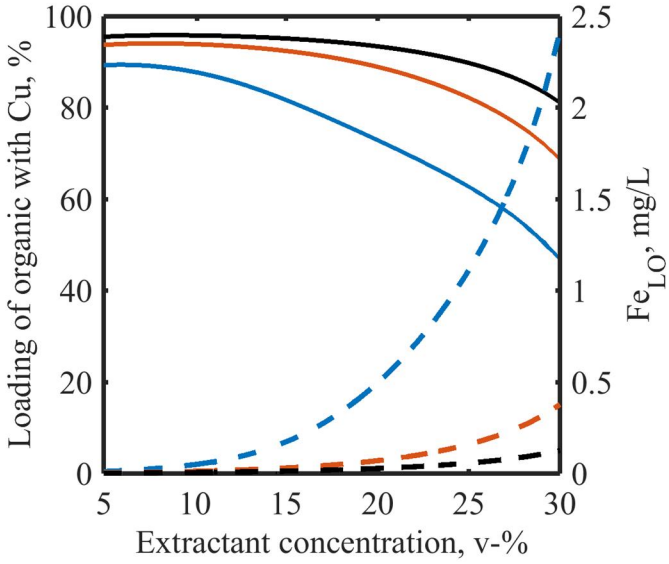

Figure 9. Effect of copper concentration in the PLS and extractant concentration in the organic phase on the performance of the copper extraction circuit (Figure 8). Solid and dashed lines are organic loading with copper and iron concentration in loaded organic, respectively. Blue lines – $C_{\mathrm{Cu}}^{\mathrm{PLS}}$ =15 g/L, red lines – $C_{\mathrm{Cu}}^{\mathrm{PLS}}$ =30 g/L, black lines – $C_{\mathrm{Cu}}^{\mathrm{PLS}}$=45 g/L. (For interpretation of the references to color in this figure legend, the reader is referred to the web version of this article.)

The small iron transfer becomes significant when the copper extraction process is run dynamically over a long time. For example, a transfer of 1 mg/L of iron per 1 m^3/h of electrolyte in the process with a 250 m^3/h flow rate of electrolyte per train results in a need to bleed about 720 m^3 per year per train according to Eq. (18). This causes losses of electrolyte additives, copper, and acid (Schlesinger *et al.*, 2011b; Thomas, 2010). Therefore, those operations that bleed for iron control should put significant focus not only on the selectivity of extractants but also on the minimization of iron transfer by determination of the optimal process parameters using equilibrium-based models.

$$F_{\mathrm{Bleed}} = F_{\mathrm{Electrolyte}} \frac{C_{\mathrm{Fe}}^{\mathrm{RE}} - C_{\mathrm{Fe,target}}^{\mathrm{RE}}}{C_{\mathrm{Fe}}^{\mathrm{LE}}}, \tag{18}$$

where F is the volumetric flow rate and $C_{\mathrm{Fe,target}}^{\mathrm{RE}}$ is the iron concentration required in rich electrolyte.

The operation of the circuit can be adjusted to favor maximum loading of the organic phase with copper to minimize the co-extraction of iron, while maintaining copper recovery at an

acceptable level. This can be done by manipulating the relative flowrates of the organic and aqueous phases in both the extraction and stripping stages of the process for fixed PLS and LE compositions and total extractant concentrations (Figure 10). Copper recovery and the percentage of copper loaded in the organic phase are opposing process performance parameters, and thus achieving maximum levels for both at the same time is not possible. Both the recovery of copper and the copper loading of the organic are more sensitive to changes of the phase ratio in stripping when the phase ratio in the extraction is high. Again, the higher the copper loading of the organic in the extraction stages, the less iron is transferred from the PLS to RE and the less bleed is required. Iron transfer and the required bleed increases with an increase in the phase ratios in both the extraction and stripping stages. High copper concentrations in the PLS along with high selectivity of the extractant result in low iron transfer and consequently low volumes of bleed for all the studied phase ratios in the extraction and stripping stages.

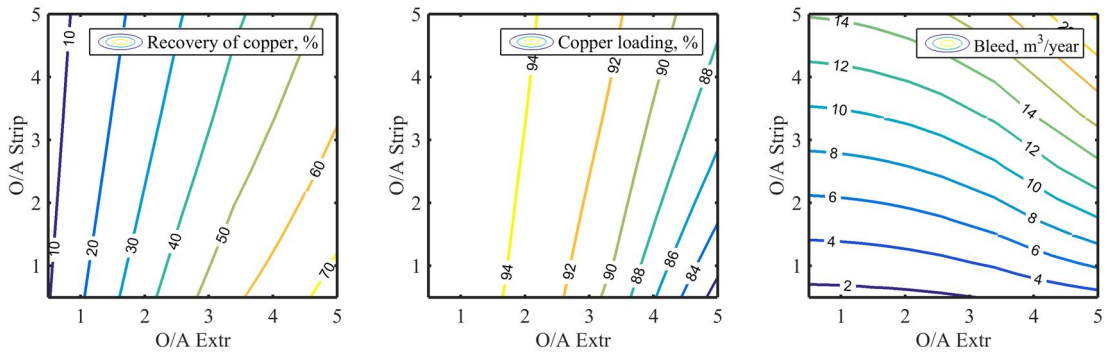

Figure 10. Performance of the extraction circuit in Figure 8 based on the phase ratios in the extraction and stripping stages. The PLS contains 45 g/L copper and the organic phase contains 25 v–% of extractant.

Performance optimization of the extraction circuit, with the aim to minimize the iron transfer from the PLS to RE and keep the copper recovery and organic loading at a desirable level, can be accomplished by solving the constrained nonlinear optimization problem, Eq. (19).

$$\min Fe_{\mathrm{RE}} = f\left(\frac{O}{A}\mathrm{extr}, \frac{O}{A}\mathrm{str}, C_{\mathrm{HR}}\right), \tag{19}$$

subject to

$$R_{\mathrm{Cu}} > R_{\mathrm{min}}$$

$$L_{\mathrm{Cu}} > L_{\mathrm{min}}$$
$$10\% < C_{HR} < 30\%,$$

where $f(\ldots)$ represents a mathematical model that calculates the equilibrium iron (III) concentration in RE, R is recovery, L is loading of the organic phase after the extraction stage, Fe_{RE} is the iron concentration in the RE, and C_{HR} is the volume percentage concentration of the extractant in the organic phase. The model, $f(\ldots)$, includes mass balance equations for copper, iron, acid and extractant, and equations for the extraction equilibrium constants for all the reactions in both extraction and stripping stages (Eqs. (5–11, 14, 17)).

For instance, with the set target loading of more than 80% and copper recovery in the liquid–liquid extraction of more than 60%, the optimum phase ratio in the extraction stages is found to be 5 and in the stripping stage 1, as the extractant concentration is 23%. Under those optimized conditions, loading is 86% and copper recovery is 67%, whereas the iron concentration in the RE increases by 5.81 μg/L in comparison to that in the LE. This operation requires only 4.2 m^3/year per train in an operation with a 250 m^3/h electrolyte flow rate per train.

The phase ratio in each extraction stage can be adjusted by internal stage recycling, and it does not affect the capacity of the total process (Kaul and Van Wormer Jr., 1985). However, mass transfer effects can influence process operation, so the steady-state of a dynamically run process may differ from the one calculated in this article based on extraction equilibrium modeling. The performance would depend on the residence time and dispersion conditions in the mixers as well as mixing effects in the settlers (Hoh *et al*., 1989). In order to improve the recovery of copper, the process performance could be enhanced by implementing an optimum series–parallel circuit configuration (Nisbett *et al.*, 2008).

4. Conclusions

A mechanistic mathematical model was developed to explain the equilibrium of the loading stage of the liquid–liquid extraction of iron (III) from concentrated aqueous sulfate solutions with a hydroxyoxime extractant in kerosene with a wide range of iron and extractant concentrations. The model was validated against an extensive amount of new experimental data using nonlinear regression analysis. The stripping stage of the liquid–liquid extraction of iron was also studied experimentally, and it was noticed that a maximum of 10% of the iron

loaded onto the organic phase could be expected to be stripped under the wide range of studied conditions.

Extraction equilibrium was modeled by an ion association model with an extended Debye–Hückel activity coefficient model to describe the speciation of the aqueous phase species and the overall interfacial extraction reaction. However, it was observed that the value of the equilibrium constant of the extraction reaction depended on the total concentration of the extractant in the organic phase. This was explained by organic phase non-ideality and was taken into account by empirical correction of the extraction equilibrium constant with a hyperbolic tangent function.

The developed model for iron extraction was combined with a previously developed model for copper extraction. The combined model was validated against experimental data, which were collected according to iteratively determined experimental conditions using the Markov chain Monte Carlo (MCMC) algorithm with the D-optimality criterion to establish the parameters of the model. The validated model was shown to excellently predict the extraction of iron (III) in the copper liquid−liquid extraction processes.

This work helps to determine the optimal process parameters for minimization of the iron transfer in the copper liquid−liquid extraction operations that bleed for iron control. The verified combined model was used to analyze the performance of a copper liquid–liquid extraction circuit that recovers copper from the PLS obtained from pressure oxidation leaching and containing 45 g/L copper, 40 g/L iron, and 20 g/L H_2SO_4. It was shown that high copper loading of the organic phase hinders the extraction of iron, and that iron extraction increases with an increase of the O/A phase ratios in both the extraction and stripping stages. With the simulations, it was shown to be possible to optimize, in terms of minimizing the iron transfer, the phase ratios (flowrates) between the organic and aqueous phases and extractant concentrations, which are among the key design parameters in the extraction process.

Acknowledgements

The work was part of DIMECC’s research program SIMP (System integrated metals processing).

Nomenclature

Abbreviations

LE	Lean electrolyte
MCMC	Markov chain Monte Carlo
MSE	Mean squared error
PLS	Pregnant leach solution
RE	Rich electrolyte
SE	Standard error

Letters

A	Parameter in regression model
I	Ionic strength
F	Flow rate
G	Number of experimental groups
HR	Protonated hydroxyoxime
J	Sensitivity of responses to parameters
K	Equilibrium constant
N	Number of experimental points in an experimental group
R	Deprotonated hydroxyoxime

Subscripts and superscripts

eq	Equilibrium
Exp	Measured experimental data
Mod	Data calculated with model

LLX	Liquid–liquid extraction
tot	Total

References

Agarwal, S., Reis, M. T. A., Ismael, M. R. C., Correia, M. J. N., Carvalho, J. M. R., 2012. Modeling of the Extraction Equilibrium of Copper from Sulfate Solutions with Acorga M5640, Solvent Extraction and Ion Exchange 30(5), 536-551.

Aminian, H., Bazin, C., 2000. Solvent extraction equilibria in copper (II)-Iron (III)-LIX984 system, Minerals Engineering 13(6), 667-672.

Casas, J. M., Alvarez, F., Cifuentes, L., 2000. Aqueous speciation of sulfuric acid-cupric sulfate solutions, Chemical Engineering Science 55(24), 6223-6234.

Casas, J. M., Crisóstomo, G., Cifuentes, L., 2005. Speciation of the Fe(II)–Fe(III)–H2SO4–H2O system at 25 and 50 °C, Hydrometallurgy 80(4), 254-264.

Cifuentes, L., Casas, J. M., Simpson, J., 2006. Temperature Dependence of the Speciation of Copper and Iron in Acidic Electrolytes, Chemical Engineering Research and Design 84(10), 965-969.

Flett, D. S., Okuhara, D. N., Spink, D. R., 1973. Solvent extraction of copper by hydroxy oximes, Journal of Inorganic and Nuclear Chemistry 35(7), 2471-2487.

Franceschini, G., Macchietto, S., 2008. Model-based design of experiments for parameter precision: State of the art, Chemical Engineering Science 63(19), 4846-4872.

Gotfryd, L., Pietek, G., 2013. Contaminants of post-leaching copper solutions and their behavior during extraction with industrial extractants, Physicochemical Problems of Mineral Processing 49(1), 133-143.

Haario, H., Laine, M., Mira, A., Saksman, E., 2006. DRAM: Efficient adaptive MCMC, Statistics and Computing 16(4), 339-354.

Hoh, Y. -., Ju, S. -., Chiu, T. -., 1989. Effect of internal recycle on mixer-settler performance, Hydrometallurgy 23(1), 105-118.

Kabugo, J., Virolainen, S., Paatero, E., Sainio, T., 2017. Liquid–liquid synthesis of oximes from carbonyl compounds: formation under neutral conditions and degradation at acidic hydrometallurgical process conditions, Journal of Chemical Technology & Biotechnology 92(6), 1446-1453.

Kaul, A., Van Wormer Jr., K. A., 1985. Effects of internal stage recycle on efficiency and performance of a mixer-settler, Industrial & Engineering Chemistry Process Design and Development 24(3), 636-646.

Liu, Y., Nam, S. -., Lee, M., 2014. Stripping of Fe(III) from the loaded mixture of D2EHPA and TBP with sulfuric acid containing reducing agents, Bulletin of the Korean Chemical Society 35(7), 2109-2113.

Molnar, R. E., Verbaan, N., 2003. Extraction of copper at elevated feed concentrations, Proceedings of the TMS Fall Extraction and Processing Conference 2, 1299-1312.

Nisbett, A., Peabody, S., Kordosky, G., 2008. Developing high-performing copper solvent-extraction circuits: strategies, concepts, and implementation, Solvent extraction: Fundamentals to industrial applications 1.

Ocaña, N., Alguacil, F. J., 1998. Solvent extraction of iron(III) by MOC-55 TD: experimental equilibrium study and demonstration of lack of influence on copper(II) extraction from sulphate solutions, Hydrometallurgy 48(2), 239-249.

Ochromowicz, K., Chmielewski, T., 2013. Solvent extraction of copper(II) from concentrated leach liquors, Physicochemical Problems of Mineral Processing 49(1), 357-367.

Parus, A., Wieszczycka, K., Olszanowski, A., 2011. Solvent extraction of iron(III) from chloride solutions in the presence of copper(II) and zinc(II) using hydrophobic pyridyl ketoximes, Separation Science and Technology 46(1), 87-93.

Ritcey, G. M., Ashbrook, A. W., 1984. Solvent Extraction : Principles and Applications to Process Metallurgy. Amsterdam; New York; New York: Elsevier Scientific Pub. Co. ; Distributors for the United States and Canada, Elsevier/North-Holland.

Rydberg, J., Cox, M., Musikas, C., Choppin, G. R., 2004. Solvent Extraction Principles and Practice .

Schlesinger, M. E., King, M. J., Sole, K. C., Davenport, W. G., 2011a. Chapter 15 - Hydrometallurgical Copper Extraction: Introduction and Leaching, in: Davenport, Mark E.Schlesinger Matthew J.King Kathryn C.Sole William G. (Ed), Extractive Metallurgy of Copper (Fifth Edition). Oxford, Elsevier, pp. 281-322.

Schlesinger, M. E., King, M. J., Sole, K. C., Davenport, W. G., 2011b. Chapter 16 - Solvent Extraction, in: Schlesinger, M. E., King, M. J., Sole, K. C., Davenport, W. G. (Eds), Extractive Metallurgy of Copper (Fifth Edition). Oxford, Elsevier, pp. 323-347.

Schlesinger, M. E., King, M. J., Sole, K. C., Davenport, W. G., 2011c. Chapter 17 - Electrowinning, in: Schlesinger, M. E., King, M. J., Sole, K. C., Davenport, W. G. (Eds), Extractive Metallurgy of Copper (Fifth Edition). Oxford, Elsevier, pp. 349-372.

Simpson, J., Navarro, P., Alguacil, F. J., 1996. Iron(III) extraction by LIX 860 and its influence on copper(II) extraction from sulphuric solutions, Hydrometallurgy 42(1), 13-20.

Smith, A. G., Tasker, P. A., White, D. J., 2003. The structures of phenolic oximes and their complexes, Coordination Chemistry Reviews 241(1–2), 61-85.

Szymanowski, J., 1993. Hydroxyoximes and Copper Hydrometallurgy. Boca Raton: CRC.

Tamminen, J., Sainio, T., Paatero, E., 2013. Intensification of metal extraction with high-shear mixing, Chemical Engineering and Processing: Process Intensification 73(0), 119-128.

Thomas, W., 2010. Solvent extraction, in: Thomas, W. (Ed), Mining Chemicals Handbook, Cytec Industries Inc, pp. 322-391.

Vasilyev, F., Virolainen, S., Sainio, T., 2017. Modeling the phase equilibrium in liquid–liquid extraction of copper over a wide range of copper and hydroxyoxime extractant concentrations, Chemical Engineering Science 171, 88-99.

Yu, S., Chen, J., Chen, C., 1989. Stripping of Fe(III) extracted by di-2-ethylhexyl phosphoric acid from sulfate solutions with sulfuric acid, Hydrometallurgy 22(1), 267-272.

Yue, G., Zhao, L., Olvera, O. G., Asselin, E., 2014. Speciation of the H2SO4–Fe2(SO4)3–FeSO4–H2O system and development of an expression to predict the redox potential of the Fe3 +/Fe2 + couple up to 150 °C, Hydrometallurgy 147–148, 196-209.

Zhang, Y., Liu, Q., Li, L., 2016. Removal of iron from synthetic copper leach solution using a hydroxy-oxime chelating resin, Hydrometallurgy 164, 154-158.